

Modulational Instabilities and Domain Walls in Coupled Discrete Nonlinear Schrödinger Equations

Z. Rapti^{1,2}, A. Trombettoni³, P. G. Kevrekidis^{1,2}, D. J. Frantzeskakis⁴, Boris A. Malomed⁵ and A. R. Bishop²

¹Department of Mathematics and Statistics, University of Massachusetts, Amherst MA 01003-4515, USA

²Center for Nonlinear Studies and Theoretical Division,

Los Alamos National Laboratory, Los Alamos, NM 87545, USA

³Istituto Nazionale per la Fisica della Materia, and Dipartimento di Fisica,
Università di Parma, Parco Area delle Scienze 7A, I-43100 Parma, Italy

⁴Department of Physics, University of Athens, Panepistimiopolis, Zografos, Athens 15784, Greece

⁵Department of Interdisciplinary Studies, Faculty of Engineering, Tel Aviv University, Tel Aviv 69978, Israel

We consider a system of two discrete nonlinear Schrödinger equations, coupled by nonlinear and linear terms. For various physically relevant cases, we derive a modulational instability criterion for plane-wave solutions. We also find and examine domain-wall solutions in the model with the linear coupling.

I. INTRODUCTION

Modulational instabilities (MIs) have a time-honored history in nonlinear wave equations. Their occurrences span areas ranging from fluid dynamics [1] (where they are usually referred to as the Benjamin-Feir instability) and nonlinear optics [2, 3] to plasma physics [4].

While earlier manifestations of such instabilities were studied in continuum systems [3, 5], in the last decade the role of the MI in the dynamics of discrete systems has emerged. In particular, the MI was analyzed in the context of the discrete nonlinear Schrödinger equation [6], a ubiquitous nonlinear-lattice dynamical model [7, 8]. More recently, it was studied in the context of weakly interacting trapped Bose-Einstein condensates (BECs), where the analytical predictions based on the discrete model [9] were found to be in agreement with the experiment [10] (see also the recent works [11, 12, 13], and recent reviews in [14, 15]). Additionally, the development of "discrete nonlinear optics" (based on nonlinear waveguide arrays) has recently provided the first experimental observation of the MI in the latter class of systems [16].

An extension of these recent works, which is relevant to both BECs in the presence of an optical-lattice potential [17, 18, 19, 21] and nonlinear optics in photorefractive crystals [22], is the case of multi-component discrete fields. These can correspond to a mixture of two different atomic species, or different spin states of the same atom, in BECs [23], or to light waves carried by different polarizations or different wavelengths in optical systems [24].

The corresponding two-component model is based on two coupled discrete nonlinear Schrödinger (DNLS) equations,

$$\begin{aligned} i \frac{\partial u_{1n}}{\partial t} &= d_1 (u_{1,n+1} + u_{1,n-1} - 2u_{1n}) + (s_{11} |u_{1n}|^2 + s_{12} |u_{2n}|^2) u_{1n} + cu_{2n}; \\ i \frac{\partial u_{2n}}{\partial t} &= d_2 (u_{2,n+1} + u_{2,n-1} - 2u_{2n}) + (s_{22} |u_{2n}|^2 + s_{21} |u_{1n}|^2) u_{2n} + cu_{1n}; \end{aligned} \quad (1)$$

This is a discrete analog of the well-known model describing nonlinear interactions of the above-mentioned light waves through self-phase-modulation and cross-phase-modulation (XPM) [3, 5]. In optics, Eqs. (1) describe an array of optical waveguides, the evolution variable being the propagation distance z (rather than time t). The choice of the nonlinear coefficients in the optical models is limited to the combinations $s_{11} = s_{22} = 3s_{12}=2$ for orthogonal linear polarizations, and $s_{11} = s_{22} = s_{12}=2$ for circular polarizations or different carrier wavelengths. In BECs, the coefficients s_{jk} in Eqs. (1), are related to the three scattering lengths a_{jk} which account for collisions between atoms belonging to the same (a_{jj}) or different (a_{jk} , $j \neq k$) species; in that case, $a_{ij} > 0$ ($a_{ij} < 0$) corresponds to the repulsive (attractive) interaction between the atoms. The linear coupling between the components, which is accounted for by the coefficient c in Eqs. (1), is relevant in optics for a case of circular polarizations in an array of optical fibers with deformed (non-circular) cores, or for linear polarizations in an array of twisted fibers [24]. On the other hand, in the BECs context, c represents the Rabi frequency of transitions between two different spin states in a resonant microwave field [20, 21].

Stimulated by the experimental relevance of the MI in discrete coupled systems, the aim of the present work is to develop a systematic study of the instability in the two-component dynamical lattices. We give an analytical derivation of the MI criteria for the case of both the nonlinear and linear coupling between the components. As a result of the analysis, we also find a novel domain-wall (DW) stationary pattern in the case of the linear coupling. The presentation is structured as follows: In the following sections we derive plane-wave solutions and analyze their stability, corroborating it with a numerical analysis of the stability intervals. We do this for the model with the linear

coupling in section II and for the one with the purely nonlinear coupling in section III. In section IV, we examine DW states in the linearly coupled lattices. Finally, the results and findings are summarized in section V.

II. THE MODEL WITH THE LINEAR COUPLING

We look for plane-wave solutions in the form

$$u_{jn} = A_j \exp[i(q_j n - \omega_j t)]; \quad j = 1, 2; \quad (2)$$

The linear coupling imposes the restrictions $q_1 = q_2 = q$ and $\omega_1 = \omega_2 = \omega$. Inserting Eq. (2) into Eqs. (1) yields

$$\begin{aligned} iA_1 &= -2d_1(\cos q - 1)A_1 + (s_{11}A_1^2 + s_{12}A_2^2)A_1 + cA_2; \\ iA_2 &= -2d_2(\cos q - 1)A_2 + (s_{12}A_1^2 + s_{22}A_2^2)A_2 + cA_1; \end{aligned} \quad (3)$$

In the particular, but physically relevant, symmetric case, with $d_1 = d_2$ and $s_{11} = s_{22}$, it follows from here that the amplitudes $A_{1,2}$ obey an equation $[(s_{11} - s_{12})A_1 A_2 - c] A_1^2 - A_2^2 = 0$, hence either of the following two relations must then be satisfied:

$$A_1 = -A_2; \quad (4)$$

$$A_1 A_2 = \frac{c}{s_{11} - s_{12}}; \quad (5)$$

In the case of Eq. (4), a nonzero solution has $A_1 = \sqrt{\frac{c}{(2d_1(\cos q - 1) + \omega - c)(s_{11} + s_{22})}}$. It exists with $s_{11} + s_{12} > 0$, provided $2d_1(\cos q - 1) + \omega - c > 0$, and with $s_{11} + s_{12} < 0$, if $2d_1(\cos q - 1) + \omega - c < 0$. When $s_{11} = -s_{12}$, one obtains solutions of the form $(A_1; A_2) = (A; A)$ with arbitrary A and $2d_1(\cos q - 1) = \omega - c$.

On the other hand, from Eq. (5), one finds that

$$A_1^2 = \frac{\omega + 2d_1(\cos q - 1)}{s_{11}} \pm \frac{1}{2} \sqrt{\frac{(\omega + 2d_1(\cos q - 1))^2 - 4c^2}{(s_{11} - s_{12})^2}} \quad (6)$$

under the restriction that this expression must be positive. When $c \neq 0$, solutions of this type exist as long as $[\omega + 2d_1(\cos q - 1)]s_{11} > 0$ (as the term under the square root is smaller in magnitude than the one outside) and the argument of the square root in (6) is non-negative. The first condition implies $\omega > 2d_1(\cos q - 1)$, for $s_{11} > 0$, and $\omega < 2d_1(\cos q - 1)$, for $s_{11} < 0$. In the case $s_{12} = 0$, Eq. (6) takes the simpler form

$$A_1^2 = (2s_{11})^{-1} [\omega + 2d_1(\cos q - 1) \pm \sqrt{(\omega + 2d_1(\cos q - 1))^2 - 4c^2}]; \quad (7)$$

For both $s_{12} = 0$ and $s_{12} = 2s_{11}$, it is necessary to impose the condition $|\omega + 2d_1(\cos q - 1)| > 2c$ for the solutions to be real. We note that these relations are similar to those derived in Ref. [21], where linearly and nonlinearly coupled systems of continuum NLS equation were considered.

It is also worth noting that the existence of two distinct uniform states with a fixed product from Eq. (5) suggests a possibility of a domain-wall (DW) solution in the model with the linear coupling. DW solutions in nonlinearly coupled discrete nonlinear Schrödinger equations were examined in Ref. [25] (following an analogy with the continuum ones of Ref. [26]). However, the present case is different, as both uniform states have non-vanishing amplitudes in both components, and, as seen from Eq. (5), the DW may exist only if $c \neq 0$. This possibility is examined in more detail in section IV.

To examine the stability of the plane waves, we substitute

$$u_{jn}(x; t) = [A_j + B_{jn}(x; t)] \exp[i(qn - \omega t)] \quad (8)$$

into Eqs. (1), to obtain a system of two coupled linearized equations for the perturbations $B_j(x; t)$. Furthermore, assuming a general solution of the above-mentioned system of the form

$$B_{jn} = \sum_j \cos(Qn - \Omega t) + i \sum_j \sin(Qn - \Omega t); \quad (9)$$

where Q and ω are the wavenumber and frequency of perturbation, we arrive at a set of four homogeneous equations for $\alpha_1, \alpha_2, \beta_1$ and β_2 . The latter have a nontrivial solution if Q and ω satisfy the dispersion relation

$$\begin{aligned} & (\alpha_1^2 - 2d_1 \sin Q \sin q)^2 - 2d_1 \cos q (\cos Q - 1) + c \frac{A_2}{A_1} - 2d_1 \cos q (\cos Q - 1) + c \frac{A_2}{A_1} - 2s_{11}A_1^2 \\ & (\alpha_2^2 - 2d_2 \sin Q \sin q)^2 - 2d_2 \cos q (\cos Q - 1) + c \frac{A_1}{A_2} - 2d_2 \cos q (\cos Q - 1) + c \frac{A_1}{A_2} - 2s_{22}A_2^2 \\ & 2c(2s_{12}A_1A_2 + c) (\alpha_1^2 - 2d_1 \sin Q \sin q) (\alpha_2^2 - 2d_2 \sin Q \sin q) - c^2 - 2d_1 \cos q (\cos Q - 1) + c \frac{A_2}{A_1} - 2s_{11}A_1^2 \\ & 2d_2 \cos q (\cos Q - 1) + c \frac{A_1}{A_2} - 2s_{22}A_2^2 - (2s_{12}A_1A_2 + c)^2 \\ & 2d_1 \cos q (\cos Q - 1) + c \frac{A_2}{A_1} - 2d_2 \cos q (\cos Q - 1) + c \frac{A_1}{A_2} - c^2 = 0: \end{aligned} \quad (10)$$

Note that in the absence of coupling, i.e., $c = s_{12} = 0$, we obtain a known relation [6]

$$(\alpha_j^2 - 2d_j \sin Q \sin q_j)^2 - 2d_j \cos q_j (\cos Q - 1) - 2d_j \cos q_j (\cos Q - 1) - 2s_{jj}A_j^2 = 0; \quad (11)$$

which gives the MI condition if the right-hand side becomes negative, i.e.,

$$d_j \cos q_j (2d_j \cos q_j \sin^2(Q/2) + s_{jj}A_j^2) < 0; \quad (12)$$

We will now consider the particular case $d_1 = d_2 = d$, the general case being technically tractable but too involved. Then, the dispersion relation (10) takes the form

$$(\alpha^2 - 2d \sin Q \sin q)^4 - (K_1 + K_2 + K_3) (\alpha^2 - 2d \sin Q \sin q)^2 + K_1K_2 - K_4 = 0; \quad (13)$$

where

$$\begin{aligned} K_1 &= 2d \cos q (\cos Q - 1) + c \frac{A_2}{A_1} - 2d \cos q (\cos Q - 1) + c \frac{A_2}{A_1} - 2s_{11}A_1^2; \\ K_2 &= 2d \cos q (\cos Q - 1) + c \frac{A_1}{A_2} - 2d \cos q (\cos Q - 1) + c \frac{A_1}{A_2} - 2s_{22}A_2^2; \\ K_3 &= 2c(2s_{12}A_1A_2 + c); \\ K_4 &= c^2 - 2d \cos q (\cos Q - 1) + c \frac{A_2}{A_1} - 2s_{11}A_1^2 - 2d \cos q (\cos Q - 1) + c \frac{A_1}{A_2} - 2s_{22}A_2^2 \\ &+ (2s_{12}A_1A_2 + c)^2 - 2d \cos q (\cos Q - 1) + c \frac{A_2}{A_1} - 2d \cos q (\cos Q - 1) + c \frac{A_1}{A_2} - c^2: \end{aligned}$$

It immediately follows from Eq. (13) that, to avoid the MI, both solutions for $(\alpha^2 - 2d \sin Q \sin q)^2$ should be positive. Taking into account the binomial nature of the equation, it is concluded that the spatially homogeneous solution is unstable if either the sum $\Sigma = K_1 + K_2 + K_3$ or the product $\Pi = K_1K_2 - K_4$ of the solutions is negative:

$$K_1 + K_2 + K_3 < 0; \quad (14)$$

$$K_1K_2 - K_4 < 0; \quad (15)$$

To proceed further, we may fix the value of the perturbation wavenumber, to investigate in what parameter region it would give rise to the MI. We illustrate this approach in Figs. 1 and 2, in which we fix $Q = \pi$ and $s_{11} = s_{22} = A_1 = A_2 = d_1 = d_2 = 1$ and vary c and s_{12} (the coefficients of the linear and XPM coupling), to examine their effect on the stability interval. From Eq. (12) we see that for these values of the parameters the modulational unstable region is $-\pi/2 < q < \pi/2$ for $s_{12} = 2.0945$. It can be inferred from the figures that c may widen the MI interval by decreasing its lower edge. On the other hand, s_{12} has a more complex effect: while making the instability interval larger by increasing its upper edge (until it reaches π), it may also open MI bands within the initially modulationally stable region (see, e.g., the lower panel of Fig. 2).

For reasons of completeness, we also illustrate nonlinear development of the MI in the coupled nonlinear lattices in some typical examples. In particular, the role of the MI in generating large-amplitude excitations in the presence of the linear coupling only ($s_{12} = 0$) is illustrated in the left panel of Fig. 3, for $c = 0.5$. In the right panel of the figure, the MI in the presence of both linear and nonlinear coupling ($c = 0.5, s_{12} = 2/3$) is shown. It is readily observed that the nonlinear coupling enhances the instability growth rate and, hence, the MI sets in earlier.

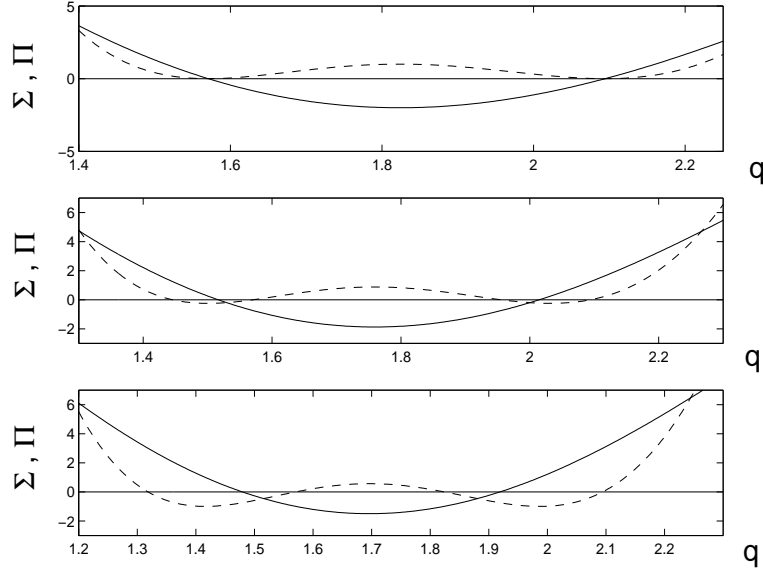


FIG. 1: The figure shows, for $s_{12} = 0$, the cases of $c = 0$ (top panel; unstable for $\omega = 2 < q < 2.0945$), $c = 0.25$ (middle panel; unstable for $1.4455 < q < 2.0945$) and $c = 0.5$ (bottom panel; unstable for $1.318 < q < 2.0945$). The solid line shows the sum and the dashed line the product of the solutions of Eq. (13). The instability takes place in intervals of the wavenumber q of the unperturbed plane-wave solution where either ω or ω (or both) are negative.

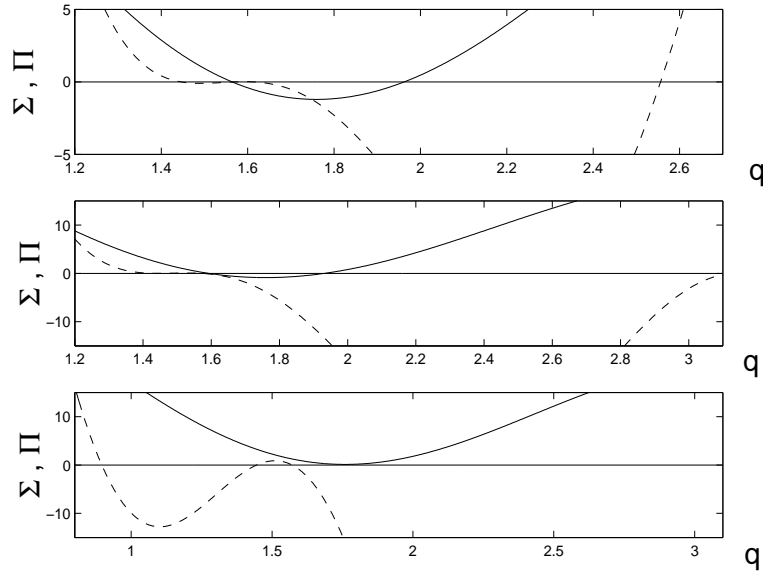


FIG. 2: Same as Fig. 1 but fixing $c = 0.25$ and varying s_{12} . The figure shows the cases of $s_{12} = 2/3$ (top panel; unstable for $1.4455 < q < 2.556$), $s_{12} = 1$ (middle panel; unstable for $\omega = 2 < q < \omega$), and $s_{12} = 2$ (bottom panel; unstable for $0.8955 < q < 1.4455$ and $\omega = 2 < q < \omega$).

III. THE CASE OF THE PURELY NONLINEAR COUPLING

A physically relevant case that we also wish to consider here is the one with only the nonlinear coupling present, i.e., $c = 0$. The corresponding dispersion relations read

$$\omega_j^2 = -2d_j(\cos q_j - 1) + s_{j1}A_1^2 + s_{j2}A_2^2; j = 1, 2: \quad (16)$$

To study the stability of the plane waves in this case, we use Eq. (8) as before, and obtain the following dispersion

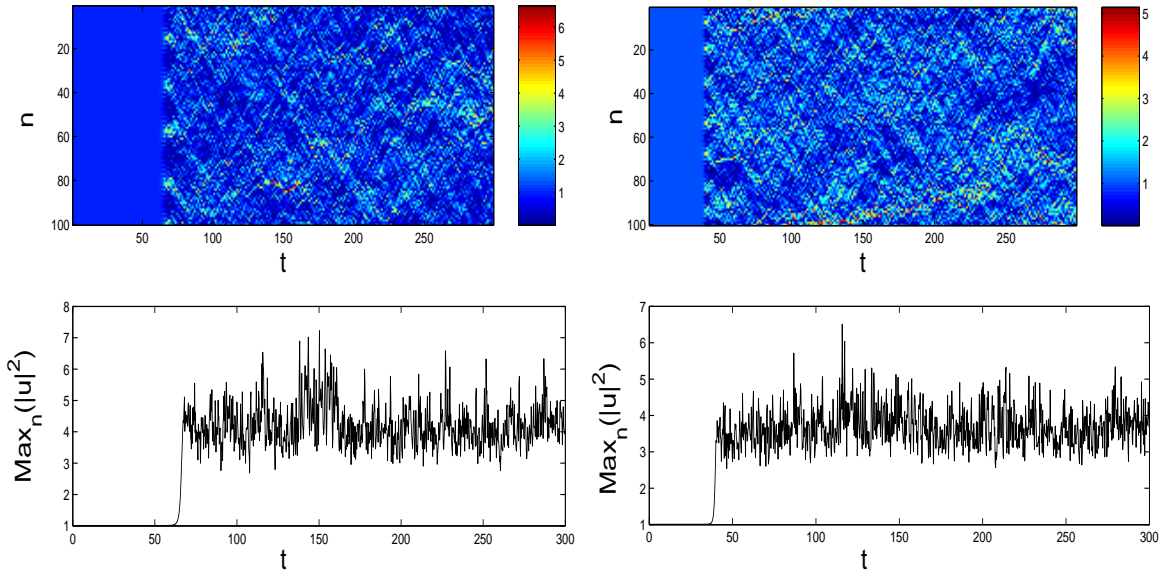


FIG. 3: Left panels: Spatio-temporal $(n;t)$ contour plots of the squared absolute value of one of the two components of the solution (top) and temporal evolution of the maximum of the solution's amplitude (bottom), $c = 0.5$, $s_{12} = 0$ and $q = -2$. Right panels: Same as the left ones but for $c = 0.5$, $s_{12} = 2/3$ and $q = -2$.

relation for the perturbation wavenumber and frequency

$$\begin{aligned} & (2d_1 \sin Q \sin q_1)^2 - 2d_1 \cos q_1 (\cos Q - 1) - 2d_1 \cos q_1 (\cos Q + 1) - 2s_{11}A_1^2 \\ & (2d_2 \sin Q \sin q_2)^2 - 2d_2 \cos q_2 (\cos Q - 1) - 2d_2 \cos q_2 (\cos Q + 1) - 2s_{22}A_2^2 \\ & 4(2s_{12}A_1A_2)^2 d_1 d_2 \cos q_1 \cos q_2 (\cos Q - 1)^2 = 0; \end{aligned} \quad (17)$$

When $s_{12} = 0$, the known result (12) for the one-component case is easily retrieved. If we let $d_1 = d_2 = d$ and $q_1 = q_2 = q$, then Eq. (17) is simplified as follows:

$$(2d \sin Q \sin q)^4 - 2K_5 (2d \sin Q \sin q)^2 + K_6 = 0; \quad (18)$$

where

$$\begin{aligned} K_5 &= 2d \cos q (\cos Q - 1) - 2d \cos q (\cos Q + 1) - (s_{11}A_1^2 + s_{22}A_2^2); \\ K_6 &= (2d \cos q (\cos Q - 1))^2 - (2d \cos q (\cos Q + 1))^2 - 2(s_{11}A_1^2 + s_{22}A_2^2)2d \cos q (\cos Q - 1) + 4A_1^2 A_2^2 (s_{11}s_{22} - s_{12}^2) \end{aligned} \quad (19)$$

We will follow the lines of the analysis outlined above for the case of the linear coupling. Examining the product and the sum of the roots of Eq. (18) for $(2d \sin Q \sin q)^2$, which now read $= K_5$ and $= K_6$, we arrive at the following MI conditions:

$$K_5 < 0; \text{ or } K_6 < 0;$$

The latter can be rewritten, respectively, as:

$$\frac{1}{2} (s_{11}A_1^2 + s_{22}A_2^2) < 2d \cos(q) \sin^2 \frac{Q}{2} < 0; \quad (20)$$

$$K < 4d \cos(q) \sin^2 \frac{Q}{2} < K_+; \quad (21)$$

with $K = \frac{s_{11}A_1^2 + s_{22}A_2^2}{(s_{11}A_1^2 + s_{22}A_2^2)^2 - 4A_1^2 A_2^2 (s_{11}s_{22} - s_{12}^2)}$. It is readily observed, in this case as well, that the coupling between the two components tends to expand the band of the MI wavenumbers with respect to the single-component case. The effect of the variation of s_{12} in this case, for fixed $s_{11} = s_{22} = A_1 = A_2 = d_1 = d_2 = 1$

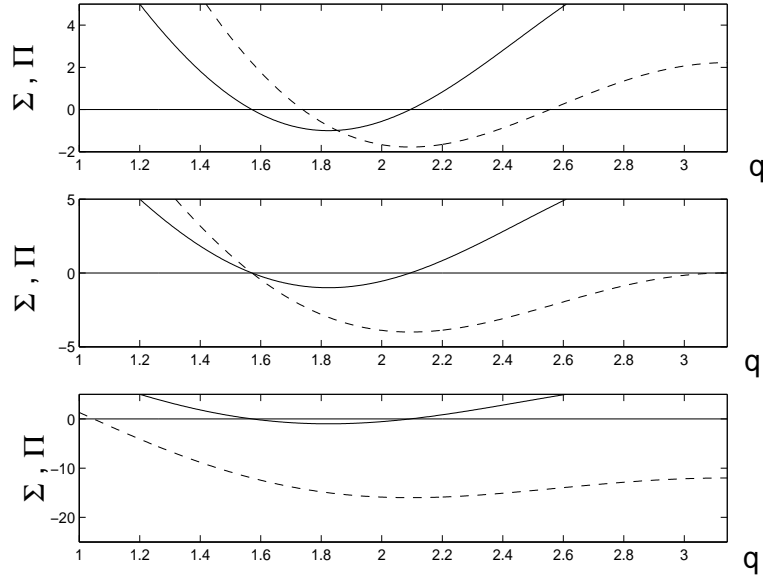


FIG. 4: Same as Fig. 2 but setting $c = 0$ and varying s_{12} . The figure shows the cases of $s_{12} = 2/3$ (top panel; unstable for $\pi/2 < q < 2.5550$), $s_{12} = 1$ (middle panel; unstable for $\pi/2 < q < \pi$), and $s_{12} = 2$ (bottom panel; unstable for $1.0472 < q < \pi$).

and $Q = \pi$, is shown in Fig. 4. Notice also that Eqs. (20) and (21) suggest multi-component generalizations of the MI criteria.

When $s_{11} = s_{22} = s$, $A_1 = A_2 = A$ and $s_{12} > 0$, the MI conditions given by Eqs. (20)–(21) can be written in a compact form,

$$sA^2 < 2d \cos(q) \sin^2(Q=2) < 0; \quad (22)$$

$$(s - s_{12})A^2 < 2d \cos(q) \sin^2(Q=2) < (s + s_{12})A^2; \quad (23)$$

From Eq. (22), we obtain that (for $Q = \pi$)

$$\frac{\pi}{2} < q < \arccos \frac{sA^2}{2d}; \quad (24)$$

while similarly from Eq. (23), it follows that

$$\arccos \frac{(s - s_{12})A^2}{2d} < q < \arccos \frac{(s + s_{12})A^2}{2d}; \quad (25)$$

Examining the latter relations in more detail, we conclude that, for $s > s_{12}$, the region of unstable wavenumbers is $\pi/2 < q < \arccos \frac{(s + s_{12})A^2}{2d}$, while, for $s < s_{12}$, Eq. (25) contains the interval of unstable q . This is illustrated for the case with $A = d = s = 1$ as a function of s_{12} in Fig. 5.

A typical example of the simulated development of the MI in the case of purely nonlinear coupling is shown in Fig. 6 for $s_{12} = 2/3$ and $q = \pi/2$.

IV. DOMAIN WALLS IN THE SYSTEM WITH THE LINEAR COUPLING

The expressions (6) for the amplitudes of the plane-wave solutions suggest a novel possibility: Focusing more specifically on the so-called anti-continuum limit of $d = 0$ (we use $d_1 = d_2 = d$) and following the path of [25], we can construct domain-wall (DW) solutions that connect the homogeneous state given by Eq. (6) with its "conjugate" state of $A_2 = c(A_1(s_{11} - s_{12}))$. Such a solution can then be continued for finite coupling, to examine its spatial profile and dynamical stability.

An example of such a solution, for the case where the nonlinear coupling is absent, is given in Fig. 7. It is observed that the solution is stable for $d < 0.033$, and it becomes unstable due to a cascade of oscillatory instabilities (through the corresponding eigenvalue quartets) for larger values of d .

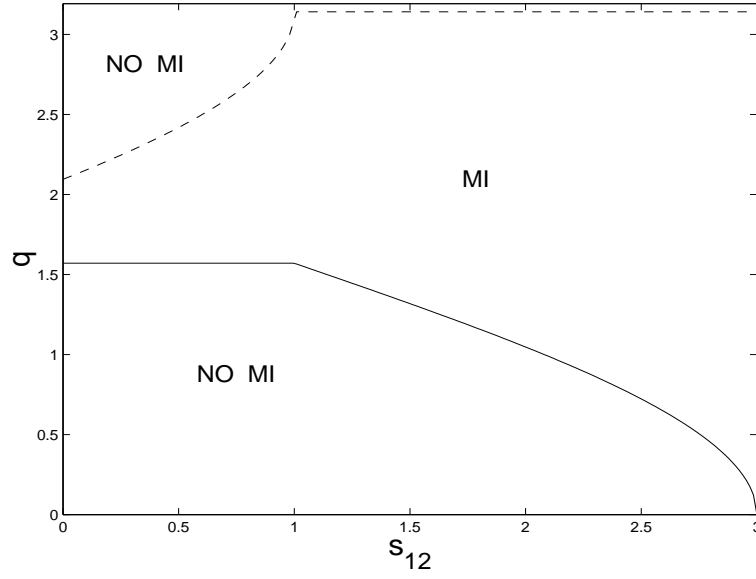


FIG . 5: The threshold wavenum bers q for the m odulational instability vs. s_{12} , as found from Eqs. (24) and (25) (for the case of $A = d = s = 1$).

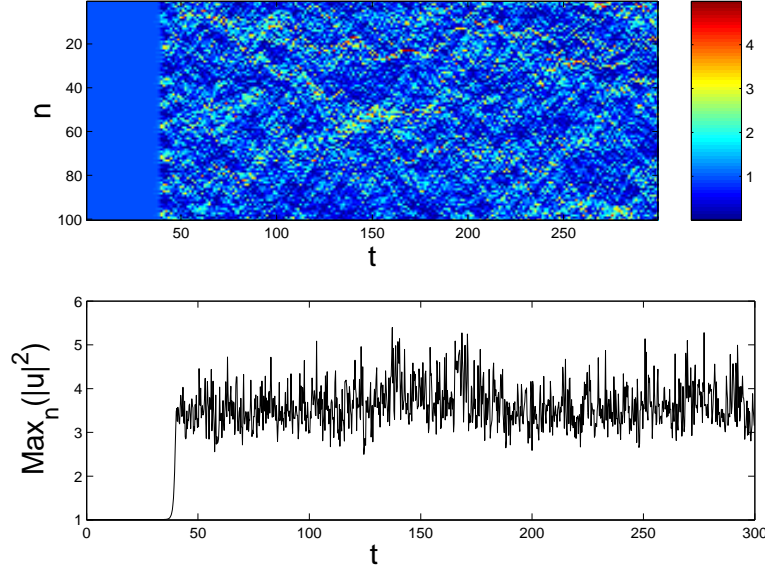


FIG . 6: Same as Fig. 3, but for $s_{12} = 2/3$ and $c = 0$ (purely nonlinear coupling); $q = 2$.

We have also examined the evolution of the DW s when they are unstable. A typical result is displayed in Fig. 8. It is seen from the bottom panel, which shows the time evolution of the solution's maximum amplitude, that growth of the oscillatory instability eventually destroys the con guration, through "lattice turbulence". This apparently chaotic evolution can be attributed to the mixing of a large number of unstable eigenmodes. The dynamics remain extremely complex despite the eventual saturation of the instability.

The increase of the nonlinear coupling constant s_{12} reduces the stability window of these solutions. In particular, the case of $s_{12} = 0.3$ is shown in Fig. 9 in which, the stability window has shrunk to $d < 0.012$.

One can also consider a modified DW , where an extra site between the two domains has equal or opposite amplitudes of the two elds. We have checked that such solutions are always unstable (due to the presence of real eigenvalue pairs), for all values of d . Still more unstable (with a larger number of unstable eigenvalues) are more sophisticated DW patterns, with additional intermediate sites inserted between the two domains.

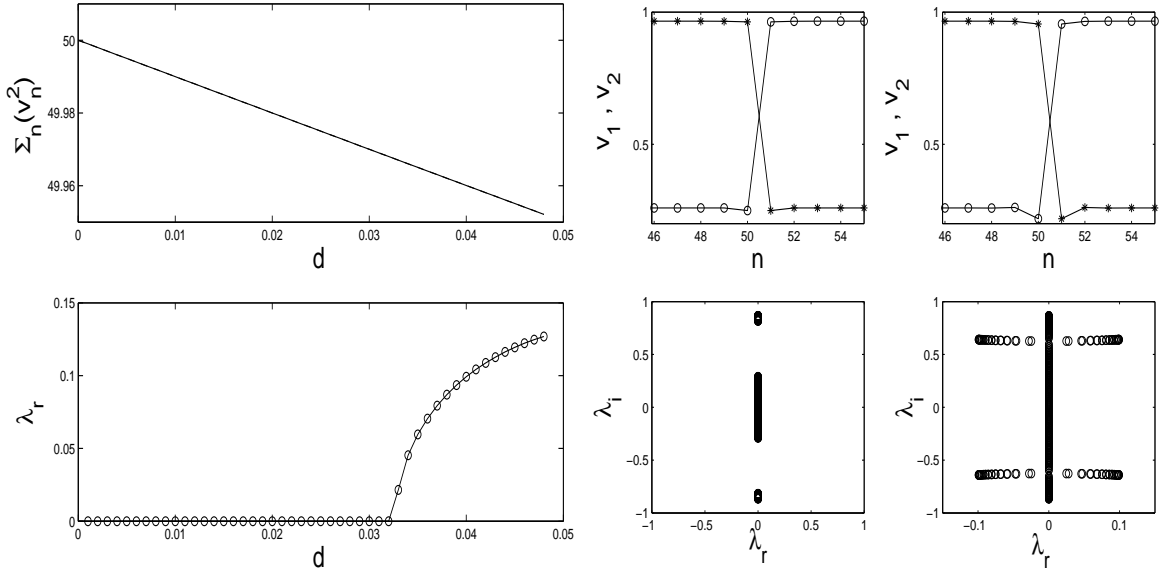


FIG. 7: The left panel (top subplot) shows the evolution of the norm of the DW solution $u_{jn} = \exp(-i|t|)v_{jn}$, as a function of the inter-site coupling constant d using continuation from the anti-continuum limit, $d = 0$. The bottom subplot shows the most unstable eigenvalue of small perturbations around the solution as a function of d . The DW becomes unstable for $d > 0.033$. The profiles of the solution (top subplots) and the respective linear-stability eigenvalues (bottom subplots) are shown in the right panel for $d = 0.01$ (stable; left subplots) and $d = 0.04$ (unstable; right subplots). The parameters are $s_{12} = 0$, $c = 0.25$, $s = 1$.

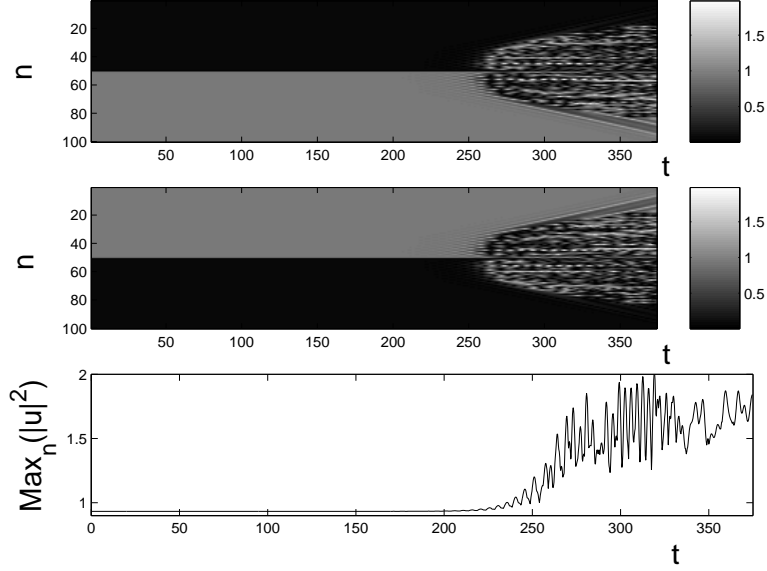


FIG. 8: The top panel shows a grayscale image of the spatio-temporal evolution of the intensity of the first field, $|u_{1n}(t)|^2$. The middle panel shows the same for the second field. The bottom panel displays the time evolution of the amplitude (the spatial maximum) of the first field.

V. CONCLUSIONS

In this work, we have examined the extension of the modulational instability (MI) concept to the case of multiple-component discrete fields. We have shown, in a systematic way, how to formulate the linear MI equations and how to extract the MI criteria. We have also followed the dynamical evolution of the instability by means of direct simulations, and have identified the effects of the linear and nonlinear couplings on the range of modulationally unstable wavenumbers. In particular, we have demonstrated that the joint action of the two couplings may give rise

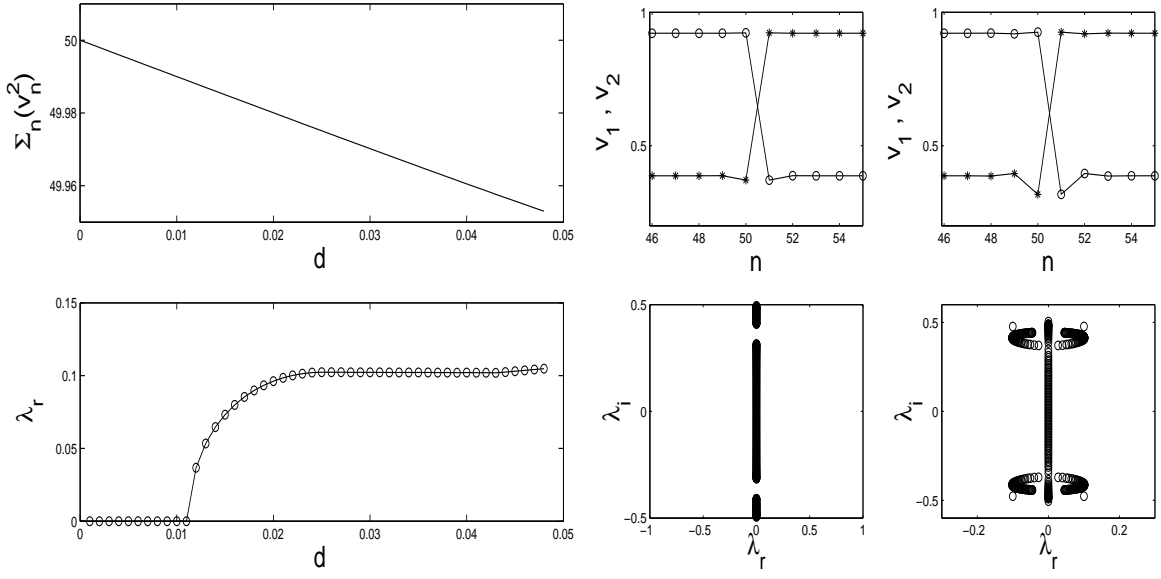


FIG. 9: Same as Fig. 7, but for $s_{12} = 0.3$. The instability sets in for $d > 0.012$.

to noteworthy features, such as opening of new MI bands on the wavenumber scale.

Additionally, the identification of a pair of conjugate uniform solutions in the two-component model has prompted us to examine domain-wall (DW) solutions between such states. We were able to demonstrate that the DWs can be linearly stable, provided that the inter-site coupling in the lattice is sufficiently weak.

From our results, it is clear that multi-component lattice models have a rich phenomenology, which is a natural addition to that of single-component ones. It would be interesting to observe the predicted features in experimental settings, including weakly coupled BECs and photonic-crystal nonlinear media.

Acknowledgements. ZR and PGK gratefully acknowledge the hospitality of the Center of Nonlinear Studies of the Los Alamos National Laboratory where part of this work was performed. PGK also acknowledges the support of NSF-DM S-0204585, NSF-CAREER and the Eppley Foundation for Research. DJF acknowledges support of the Special Research Account of University of Athens. The work of BAM was supported, in a part, by the Israel Science Foundation through the grant No. 8006/03. Research at Los Alamos is performed under the auspices of the US-DOE.

-
- [1] T. B. Benjamin and J. E. Feir, *J. Fluid. Mech.* **27**, 417 (1967).
 - [2] L. A. Ostrovskii, *Sov. Phys. JETP* **24**, 797 (1969).
 - [3] G. P. Agrawal, *Nonlinear Fiber Optics*. Academic Press, San Diego, CA, 1995.
 - [4] T. Taniuti and H. Washimi, *Phys. Rev. Lett.* **21**, 209 (1968); A. Hasegawa, *Phys. Rev. Lett.* **24**, 1165 (1970).
 - [5] A. Hasegawa and Y. Kodama, *Solitons in Optical Communications*, Clarendon Press (Oxford 1995)
 - [6] Yu. S. Kivshar and M. Peyrard, *Phys. Rev. A* **46**, 3198 (1992).
 - [7] D. N. Christodoulides and R. I. Joseph, *Opt. Lett.* **13**, 794 (1988)
 - [8] For recent reviews see, e.g., P. G. Kevrekidis, K. Rasmussen, and A. R. Bishop, *Int. J. Mod. Phys. B*, **15**, 2833 (2001); J. C. Eilbeck and M. Johansson, { *Proc. of the 3rd Conf. Localization & Energy Transfer in Nonlinear Systems* (June 17-21 2002, San Lorenzo de El Escorial Madrid), ed. L. Vazquez et al. (World Scientific, New Jersey, 2003), p. 44 (arXiv:nl/PS/0211049).
 - [9] A. Smirzi, A. Trombettoni, P. G. Kevrekidis, and A. R. Bishop, *Phys. Rev. Lett.* **89**, 170402, (2002)
 - [10] F. S. Cataliotti, L. Fallani, F. Ferlaino, C. Fort, P. Maddaloni and M. Inguscio, *New J. Phys.* **5**, 71 (2003).
 - [11] V. V. Konotop and M. Salerno *Phys. Rev. A* **65**, 021602 (2002).
 - [12] M. M. Achholm, A. Nicolin, C. J. Pethick and H. Smith, *Phys. Rev. A* **69** (2004) 043604.
 - [13] L. Fallani et al., *cond-mat/0404045*.
 - [14] F. Kh. Abdullaev, S. A. Damanyan and J. Gamier, *Progr. Opt.* **44**, 303 (2002).
 - [15] P. G. Kevrekidis and D. J. Frantzeskakis, *Mod. Phys. Lett. B* **18**, 173 (2004).
 - [16] J. Meier et al., *Phys. Rev. Lett.* **92**, 163902 (2004).
 - [17] O. Mandel, M. Greiner, A. Widera, T. Rom, T. W. Hansch, and I. Bloch, *Phys. Rev. Lett.* **91**, 010407 (2003).
 - [18] B. Deconinck, J. N. Kutz, M. S. Patterson, and B. W. Warner, *J. Phys. A: Math. Gen.* **36**, 5431 (2003).

- [19] P. G. Kevrekidis, G. Theodorakis, D. J. Frantzeskakis, B. A. Malomed and R. Carretero-Gonzalez, *Eur. Phys. J. D: At. Mol. Opt. Phys.* **28**, 181 (2004).
- [20] R. J. Ballagh, K. Burnett, and T. F. Scott, *Phys. Rev. Lett.* **78**, 1607 (1997); J. Williams, R. W. Alser, J. Cooper, E. Cornell, and M. Holland, *Phys. Rev. A* **59**, R31 (1999); P. Ohberg and S. Stenholm, *Phys. Rev. A* **59**, 3890 (1999).
- [21] M. A. Porter, P. G. Kevrekidis, and B. A. Malomed, *nl in CD/0401023*, *Physica D* **196** (2004) 106.
- [22] For recent work see, e.g., J. W. Fleischer et al., *Phys. Rev. Lett.* **92**, 123904 (2004); D. N. Neshev et al., *Phys. Rev. Lett.* **92**, 123903 (2004).
- [23] See, e.g., C. J. Myatt et al., *Phys. Rev. Lett.* **78**, 586 (1997); D. S. Hall et al., *Phys. Rev. Lett.* **81**, 1539 (1998); D. M. Stamper-Kurn et al., *Phys. Rev. Lett.* **80**, 2027 (1998); G. M. odugno et al., *Science* **294**, 1320 (2001); M. Mudrich et al., *Phys. Rev. Lett.* **88**, 253001 (2002); M. Trippenbach et al., *J. Phys. B* **33**, 4017 (2000); S. Coen and M. Haelterman, *Phys. Rev. Lett.* **87**, 140401 (2001); P. Ohberg and L. Santos, *Phys. Rev. Lett.* **86**, 2918 (2001); Th. Busch and J. R. Anglin, *Phys. Rev. Lett.* **87**, 010401 (2001).
- [24] For a recent discussion of the various optical applications see, e.g., J. Hudock et al., *Phys. Rev. E* **67**, 056618 (2003).
- [25] P. G. Kevrekidis et al., *Phys. Rev. E* **67**, 036614 (2003).
- [26] B. A. Malomed, *Phys. Rev. E* **50**, 1565 (1994).